J. Plasma Phys. (2017), *vol.* 83, 905830102
doi:10.1017/S0022377816001239

Cyclotron auto resonance maser and free electron laser devices: a unified point of view

E. Di Palma[1],†, E. Sabia[1], G. Dattoli[1], S. Licciardi[2] and I. Spassovsky[1]

[1]ENEA – Frascati Research Center, Via Enrico Fermi 45, 00044, Frascati, Rome, Italy

[2]University of Catania, Department of Mathematics, Via Santa Sofia, 64, 95125 Catania, Italy

(Received 8 July 2016; revised 12 December 2016; accepted 13 December 2016)

We take advantage of previous research in the field of cyclotron auto resonance maser (CARM) and undulator-based free electron laser (U-FEL) sources to establish a common formalism for the relevant description of the underlying physical mechanisms. This strategy is aimed at stressing the deep analogies between the two devices and at providing a practical tool for their study based on the use of well-tested scaling formulae developed independently for the two systems.

Key words: plasma diagnostics, plasma heating, plasma interactions

1. Introduction

The theory of cyclotron auto resonance maser (CARM) and undulator-based free electron laser (U-FEL) devices is well established. The underlying physics is satisfactorily well described by the theoretical formulations dating back more than thirty years. The numerical codes originated by these analyses are powerful working tools, useful to analyse experimental data and to fix the design details of new devices.

Even though different, in many constructive details, the physical mechanism underlying the operation of the CARM (Nusinovich 2004) and U-FEL (Saldin, Schneidmiller & Yurkov 2000) traces back to the power transfer from the electron beam (e-beam) to a high-frequency electromagnetic field, through a klystron-like mechanism, which is the common ancestor for these families of free electron coherent generators.

The possibility of establishing a common thread between these devices has been discussed in many authoritative papers in the past see e.g. Gapanov *et al.* (1967), Bratman, Ginzburg & Petelin (1979), Fliflet (1986). More recently (Ceccuzzi *et al.* 2015) some of the present authors used the theoretical analyses developed by different authors (Gapanov *et al.* 1967; Bratman *et al.* 1979, 1981; Fliflet 1986; Nusinovich, Latham & Li 1994) to provide the translation of the CARM into U-FEL formalism by means of the analytical formulae summarized in Dattoli, Ottaviani & Pagnutti (2007), providing the back-bone of the code named PARSIFEL (Artioli *et al.* 2012).

The pathway leading to PARSIFEL is the result of an effort aimed at merging analytical formulae derived from U-FEL theory and scaling relations benchmarked through the available numerical codes, to get an accurate, reliable and semi-analytical

† Email address for correspondence: emanuele.dipalma@enea.it

physical model of the code devoted to preliminary design of FEL operating in different configurations.

In this paper we take a step further towards an extension of a PARSIFEL-like concept to CARM devices.

Regarding CARM we keep, as reference papers, those listed in Gapanov *et al.* (1967), Bratman *et al.* (1979), Bratman *et al.* (1981), Fliflet (1986), Nusinovich *et al.* (1994) and for U-FEL (Saldin *et al.* 2000) we have referred to the lines developed in the past by different authors and summarized in books and review articles, a partial list of which is reported in Marshall (1985), Luchini & Motz (1990), Colson (1990), Dattoli, Renieri & Torre (1993).

In this introductory section, we will provide a quick review of the results obtained in Ceccuzzi *et al.* (2015) and present the formalism we will adopt in the forthcoming parts of the paper.

We note that in a CARM–FEL a moderately relativistic continuous waveform e-beam, moves, inside a waveguide under the influence of an axial magnetic field, executing a helical path with a cyclotron frequency $\Omega_0 = eB/m_e$, 'e' being the electron charge, 'me' the electron mass and 'B' the magnetic field.

The kinematical variables of the electron beam are specified by the longitudinal (v_z) and transverse ($v_\perp$) velocity components, linked to the relativistic factor γ by:

$$\left.\begin{aligned} \beta_z^2 + \beta_\perp^2 &= 1 - \frac{1}{\gamma^2}, \\ \beta_{z,\perp} &= \frac{v_{z,\perp}}{c}, \\ \alpha &= \frac{v_\perp}{v_z}, \end{aligned}\right\} \tag{1.1}$$

where α is the so called pitch factor.

The electrons, with longitudinal velocity v_z, interact with a co-propagating electromagnetic field characterized by a wavevector k_z, linked to the wavephase velocity v_p with the operational angular frequency (omega) by:

$$k_z = \frac{\omega}{v_p}. \tag{1.2}$$

In the case of magnetic undulators the electrons (with the same aforementioned kinematical attributes) enter into an alternating (transverse static) magnetic field with period λ_u, where execute transverse oscillations.

In this case the emission process is not constrained by any waveguide condition, therefore no complications arise with the wavephase velocity.

The two devices can be considered 'topologically equivalent', therefore useful analogies can be defined after an appropriate analysis of the emission mechanisms.

The derivation of the wavelength, characterizing the emission process inside the undulator, can be obtained using a fairly simple argument. The difference in velocities is such that, after one undulator period, the radiation has slipped ahead of the electron beam by the so called slippage length:

$$\delta = (c - v_z)\,\frac{\lambda_u}{c} = (1 - \beta_z)\;\lambda_u. \tag{1.3}$$

Since δ is linked to the phase advance of the electromagnetic wave with respect to the electrons, constructive interference of the wavefront of the emitted radiation at the next undulator period is ensured if:

$$\delta = \lambda, \tag{1.4}$$

where λ is the wavelength of the co-propagating field.

https://doi.org/10.1017/S0022377816001239 Published online by Cambridge University Press

The last two equations yield the FEL resonance condition, which can also be cast in the form:

$$\left.\begin{aligned}\omega = \frac{2\pi\, c}{\lambda} = \frac{\omega_u}{1-\beta_z},\\ \omega_u = \frac{2\,\pi\, c}{\lambda_u}.\end{aligned}\right\} \tag{1.5}$$

To this aim we note that the electrons, with relativistic factor γ, enter inside the undulator, where on account of the Lorenz force induced by the magnetic field they acquire a transverse velocity component $\beta_\perp$, the longitudinal velocity can accordingly be written, using (1.1), as

$$\left.\begin{aligned}\beta_z = \sqrt{1-\frac{1}{\gamma_z^2}},\\ \gamma_z = \frac{\gamma}{\sqrt{1+\bar{\alpha}^2}},\\ \bar{\alpha} = \gamma\beta_\perp.\end{aligned}\right\} \tag{1.6}$$

If the relativistic factor is large enough to allow a series expansion of the square root, in the first of the equations (1.6), at the lowest order in $1/\gamma_z^2$, we find:

$$\omega \cong 2\,\frac{\gamma^2}{1+\bar{\alpha}^2}\omega_u. \tag{1.7}$$

The previous derivation can be extended to CARM by noting that the relevant 'resonance' condition, can be determined by using the same argument as before about constructive interference, which occurs whenever the accumulated slippage between radiation and electrons, in a helix period, equals the wavelength Λ. By taking into account that the link between helix period and guiding magnetic field is provided by

$$\Lambda = \frac{2\pi c}{\Omega}. \tag{1.8}$$

We impose the resonance condition as

$$(v_p - v_z)\,\frac{\Lambda}{c} = \lambda, \tag{1.9}$$

where we have used the phase velocity v_p to determine the radiation electron slippage.

The previous equation (1.9) can also be written in the more familiar form:

$$\omega = \frac{\Omega_0}{\gamma} + k_z v_z. \tag{1.10}$$

The above equation has been derived by using a kinematic argument and the analogy with U-FEL has been the pivotal element of the discussion. The physical origin of the previous identity can however be understood on the basis of different arguments, involving e.g. momentum (electron and fields) conservation (Bratman *et al.* 1981).

https://doi.org/10.1017/S0022377816001239 Published online by Cambridge University Press

We can further elaborate the previous identities, denoting by ω_R the resonant frequency, we obtain, from (1.10)

$$\left.\begin{aligned}\omega_R &= \frac{\Omega}{1-\dfrac{v_z}{v_p}},\\ \Omega &= \frac{\Omega_0}{\gamma}.\end{aligned}\right\} \tag{1.11}$$

It is worth stressing that, since the phase velocity is dependent on the field frequency, (1.11) is not an explicit solution for ω but only an approximation.

Before establishing further the analogy between U-FEL and CARM, we discuss the physical meaning of the previous equations.

The CARM resonance condition can also be derived by requiring the matching between (1.10) and the waveguide dispersion relation:

$$\omega^2 = c^2(k_\perp^2 + k_z^2), \tag{1.12}$$

where $k_\perp$ is the transverse mode wavenumber, associated with the cutoff frequency $\omega_c = ck_\perp$. It is easily checked that, from (1.10) and (1.11), one gets

$$\omega_\pm \cong \frac{\Omega}{1 \mp \dfrac{\beta_z}{\beta_p}}. \tag{1.13}$$

The down shifted intersection, yielding the gyrotron mode (Nusinovich 2004), will not be considered in the following.

The upper shifted counterpart ω_+ is the resonant (CARM) frequency and to better understand its role it will be rewritten as:

$$\left.\begin{aligned}\omega_R \cong \frac{\Omega}{1-\dfrac{\beta_z}{\beta_p}} &= \frac{\Omega}{1-\dfrac{1}{\beta_p}\sqrt{1-\dfrac{1}{\gamma_z^2}}} \cong 2\beta_p\,\gamma_z^2\Omega,\\ \gamma_z &= \frac{\gamma}{\sqrt{1+\bar{\alpha}^2}},\end{aligned}\right\} \tag{1.14}$$

based upon the assumption that γ_z be sufficiently large that $\sqrt{1-(1/\gamma_z^2)} \cong 1-(1/2\,\gamma_z^2)$ and $\beta_p \simeq 1$.

Equation (1.14) accounts for the frequency Doppler up-shift mechanism, characterizing most free electron devices.

It is important to emphasize that, at least formally, we have established so far an important analogy between CARM and U-FEL, namely $\Lambda \leftrightarrow \lambda_u$, which justifies the remark that the two devices are topologically equivalent.

The role of the transverse velocity needs a more accurate comment. In the case of the U-FEL the transverse component, induced by the Lorenz force, is the tool allowing the coupling with the co-propagating electromagnetic (transverse) field. The explicit dependence of $\bar{\alpha}$ on the undulator parameters is provided by:

$$\left.\begin{aligned}\bar{\alpha} &= \frac{K}{\sqrt{2}},\\ K &\propto e\,B_0\lambda_u.\end{aligned}\right\} \tag{1.15}$$

https://doi.org/10.1017/S0022377816001239 Published online by Cambridge University Press

In the case of the CARM the role of the transverse velocity component is the same as that of the undulator strength in the FEL undulator.

This velocity component should be induced during the electron beam preparatory phase, before the injection into the cavity.

What we have described so far are the physical conditions underlying the 'spontaneous' emission, which is the prerequisite for the onset of the coherent emission process. As is well known, it occurs via the bunching mechanism. The interaction of the electrons with the cavity mode electric field determines their energy modulation, which transforms into a density modulation, followed by a coherent radio frequency (RF) emission when the electrons are bunched on a scale comparable to the RF electric field wavelength.

This description encompasses all devices of FEL type, CARM is however made peculiar by the fact that the auto resonance is guaranteed even near saturation because any increase of Ω is balanced by a corresponding decrease of the longitudinal velocity*.

A further important quantity, characterizing U-FEL, is the number of undulator periods, which is associated with the oscillations executed by an electron while travelling inside the undulator. In the case of CARM it can be linked to the number of helical turns of the electrons inside the magnet. Accordingly we get

$$\left.\begin{aligned} \Omega \frac{L}{\beta_z c} &= 2\,\pi\, N, \\ N &\cong \frac{L}{\Lambda}, \end{aligned}\right\} \tag{1.16}$$

where L is the interaction length.

So far we have explained the main elements of our approach and in the following section we will see how the correspondences we have established may provide an effective tool to evaluate the CARM operation.

2. The CARM small signal theory

In this section we will develop further the analogy with U-FEL by showing that the equation describing the CARM field evolution in the linear regime can be written by taking advantage of the simplified expression which is valid in the former case.

In the analysis of the previous section we did not include any consideration regarding the interaction of the wave with the e-beam. The dispersion relation in (1.10)–(1.11) is appropriate for the 'cold' waveguide condition, which merely applies to the kinematic of the mode propagation.

The CARM dynamics, associated with the radiation intensity growth in the waveguide, undergoes different phases characterized by the amount of the field power density.

The weak coupling regime is characterized by a power level well below the threshold of the saturation intensity (namely the power density halving the small signal gain) and the relevant theory can be treated using perturbative methods and, to some extent, useful information can be drawn using analytical means. A significant result from such a treatment is the derivation of a modified dispersion relation

*The efficiency enhancement is induced in undulator-based FELs by tapering the undulator, by reducing e.g. the undulator period, in order to maintain the resonance condition in (1.5) fixed when β_z decreases, thus realizing the effect naturally entangled with the CARM operating mechanism.

https://doi.org/10.1017/S0022377816001239 Published online by Cambridge University Press

including the interaction of the electrons with the waveguide modes. According to Chen & Wurtele (1991), and Friedman *et al.* (2012) we find

$$\frac{\omega^2}{c^2} = (k_\perp^2 + k_z^2) + \tilde{\varepsilon}\frac{2k_\perp^2\,(\omega - k_z v_z)}{\left(\omega - \dfrac{\Omega_0}{\gamma} - k_z v_z\right)} - \tilde{\varepsilon}\frac{k_\perp^2\beta_\perp^2\left(\omega^2 - c^2k_z^2\right)}{\left(\omega - \dfrac{\Omega_0}{\gamma} - k_z v_z\right)^2}, \tag{2.1}$$

where $\tilde{\varepsilon}$ plays the role of coupling parameter. It depends on the beam current and on the geometrical parameters of the waveguide itself and will be specified later in this section. In (2.1) the terms containing the coupling ε are those ruling the field electron evolution, we simplify the analysis by neglecting the first because the second is dominating near the resonance. We are therefore left with

$$\frac{\omega^2}{c^2} = (k_\perp^2 + k_z^2) - \varepsilon\frac{k_\perp^2\left(\omega^2 - c^2k_z^2\right)}{\left(\omega - \dfrac{\Omega_0}{\gamma} - k_z v_z\right)^2}, \tag{2.2}$$

in which we have set $\varepsilon = \tilde{\varepsilon}\beta_\perp^2$.

The previous identity is the crucial element of the forthcoming discussion and, for later convenience, we set

$$\left.\begin{aligned} \tilde{k}_z &= k_z + \delta_{k_z}, \\ k_z &= \left(\frac{\omega^2}{c^2} - k_\perp^2\right)^{1/2} = \frac{\gamma\,\omega - \Omega_0}{\gamma\,v_z}, \end{aligned}\right\} \tag{2.3}$$

with δ_{k_z} representing the deviation of the field longitudinal wavevector induced by the coupling with the electrons. Inserting (2.3) into (2.2) we find that δ_{k_z} is specified by the following fourth degree algebraic equation

$$\beta_z^2\delta_{k_z}^4 + 2\,\beta_z^2 k_z\delta_{k_z}^3 + \varepsilon k_\perp^2\delta_{k_z}^2 + 2\,\varepsilon\,k_\perp^2\,k_z\delta_{k_z} - \varepsilon\,k_\perp^4 = 0. \tag{2.4}$$

The roots of the above equation specifies the evolution of the CARM field amplitude along the coordinate z, according to

$$E\,(z) \propto \sum_{j=1}^{4} e_j e^{(\delta_{k_z})_j z}, \tag{2.5}$$

where j refers to the roots of (2.4) and e_j are integration constants, fixed by the conditions

$$\left.\begin{aligned} E\,(0) &= 1, \\ \left(\left(\frac{\mathrm{d}}{\mathrm{d}z}\right)^k E(z)\right)_{z=0} &= 0, \\ k &= 1,\,2,\,3. \end{aligned}\right\} \tag{2.6}$$

The linearized field growth along the longitudinal coordinate can accordingly be obtained by plotting $|E(z)|^2$ as shown in figure 1.

https://doi.org/10.1017/S0022377816001239 Published online by Cambridge University Press

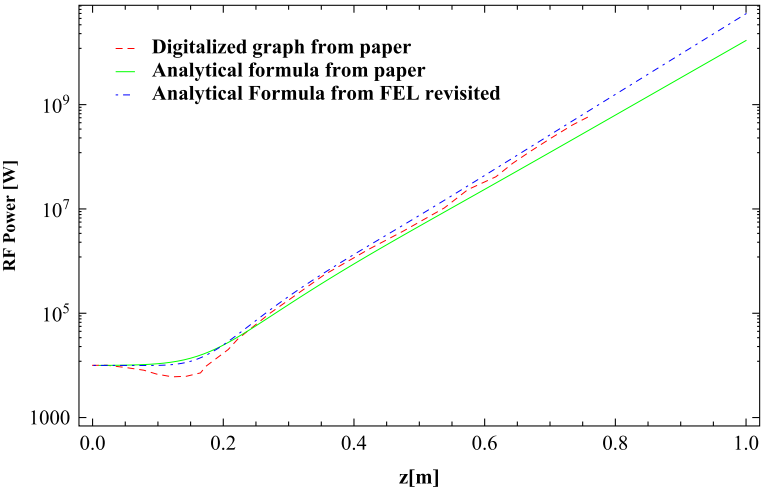

FIGURE 1. Comparison between U-FEL (blue) and CARM (green) intensity growth curves in a small signal regime with the result reported in Chen & Wurtele (1991).

The evolution curve exhibits the well-known shape, characterizing also the high gain U-FEL operating mode, namely an initial phase during which the electrons acquire the bunching, allowing the second phase, characterized by a linear (in logarithmic scale) growth with a characteristic gain length l_g. In the case of CARM such a quantity is specified by (Chen & Wurtele 1991)

$$l_g^{-1} = 2\Gamma = \sqrt{3}\left[\frac{\varepsilon\, k_\perp^4}{16\, k_z \beta_z^2}\right]^{1/3}. \tag{2.7}$$

Let us now invoke the analogy with the U-FEL, whose gain length is defined as (Dattoli *et al.* 2007)

$$l_g = \frac{\lambda_u}{4\,\pi\,\sqrt{3}\,\rho}, \tag{2.8}$$

with ρ being the Pierce parameter linked to the small signal gain coefficient g_0 by the identity (Dattoli *et al.* 2007)

$$\rho = \frac{(\pi\, g_0)^{1/3}}{4\,\pi\, N}. \tag{2.9}$$

The use of the correspondences established in the previous section and the comparison between (2.7), (2.8) allows the following identification

$$\rho = \frac{\Lambda\,\Gamma}{4\,\pi\,\sqrt{3}}. \tag{2.10}$$

The dependence of the U-FEL field amplitude on the longitudinal coordinate has been shown to be provided by (Dattoli *et al.* 2007)†.

†Equation (2.11), obtained from the U-FEL third-order dispersion equation solved using the Cardan rule is reported in Dattoli *et al.* (2007), we must stress that an analogous expression has also been derived by Professor H. Fang in an unpublished note, written prior to 1990.

https://doi.org/10.1017/S0022377816001239 Published online by Cambridge University Press

$$a(\tau) = \frac{a_0}{3\,(\nu+p+q)}\,\mathrm{e}^{-(2/3)\,\mathrm{i}\nu\,\tau}\left\{(-\nu+p+q)\,\mathrm{e}^{-\mathrm{i}/3\,(p+q)\,\tau} + 2\,(2\,\nu+p+q)\,\mathrm{e}^{\mathrm{i}/6\,(p+q)\,\tau}\right.$$
$$\left.\times\left[\cosh\left(\frac{\sqrt{3}}{6}\,(p-q)\,\tau\right)+\mathrm{i}\frac{\sqrt{3}\,\nu}{p-q}\sinh\left(\frac{\sqrt{3}}{6}\,(p-q)\,\tau\right)\right]\right\}, \tag{2.11a}$$

$$p = \left[\tfrac{1}{2}(r+\sqrt{d})\right]^{1/3}, \tag{2.11b}$$

$$q = \left[\tfrac{1}{2}(r-\sqrt{d})\right]^{1/3}, \tag{2.11c}$$

$$r = 27\,\pi\,g_0 - 2\,\nu^3, \tag{2.11d}$$

$$d = 27\,\pi\,g_0[27\,\pi\,g_0 - 4\,\nu^3]. \tag{2.11e}$$

The various parameters entering the above expression are recognized as

$$\nu \equiv \text{detuning parameter}, \tag{2.12a}$$

$$z \equiv \text{longitudinal coordinate}, \tag{2.12b}$$

$$L \equiv N\,\lambda_u \equiv \text{interaction length}, \tag{2.12c}$$

$$\tau \equiv \text{dimensionless time}. \tag{2.12d}$$

The correspondence with the CARM variables is obtained by defining the normalized detuning $\bar{\nu}$ parameter as

$$\bar{\nu} = \frac{\nu}{(27\pi\,g_0)^{1/3}}, \tag{2.13}$$

and then by casting, using the relations (2.7)–(2.9), the dimensionless time in the form

$$\tau = \frac{z}{L} = \frac{z}{Nl_g 4\pi\sqrt{3}\rho} = \frac{2\Gamma z}{\sqrt{3}(\pi g_0)^{1/3}}, \tag{2.14}$$

thus finally ending up with

$$\nu\tau = 2\sqrt{3}\Gamma\bar{\nu}z. \tag{2.15}$$

The complex amplitude (2.11) can now be assumed to be a function of the normalized detuning parameter $\bar{\nu}$ and of the inverse gain length, Γ, which will be exploited to describe the small signal growth of the radiation field amplitude, namely

$$a(z,\,\Gamma,\,\bar{\nu}) = \frac{a_0}{3}\mathrm{e}^{-\mathrm{i}(4\Gamma\bar{\nu}z/\sqrt{3}\beta_z)}\cdot\left\{A_1\mathrm{e}^{-\mathrm{i}(2\Gamma z A_3^{(+)}/\sqrt{3})} + 2A_2\mathrm{e}^{\mathrm{i}(\Gamma z A_3^{(+)}/\sqrt{3})}\right.$$
$$\left.\cdot\left[\cosh(\Gamma z A_3^{(-)}) + \imath\frac{\sqrt{3}\bar{\nu}}{A_3^{(+)}}\sinh(\Gamma z A_3^{(-)})\right]\right\}, \tag{2.16}$$

with

$$A_1 := A_1(\bar{\nu}) = \frac{(-\nu+p+q)}{\nu+p+q}$$
$$= \frac{\left(\sqrt[3]{1-2\bar{\nu}^3+\sqrt{1-4\bar{\nu}^3}}+\sqrt[3]{1-2\bar{\nu}^3-\sqrt{1-4\bar{\nu}^3}}-\sqrt[3]{2}\bar{\nu}\right)}{\left(\sqrt[3]{1-2\bar{\nu}^3+\sqrt{1-4\bar{\nu}^3}}+\sqrt[3]{1-2\bar{\nu}^3-\sqrt{1-4\bar{\nu}^3}}+\sqrt[3]{2}\bar{\nu}\right)}, \tag{2.17a}$$

https://doi.org/10.1017/S0022377816001239 Published online by Cambridge University Press

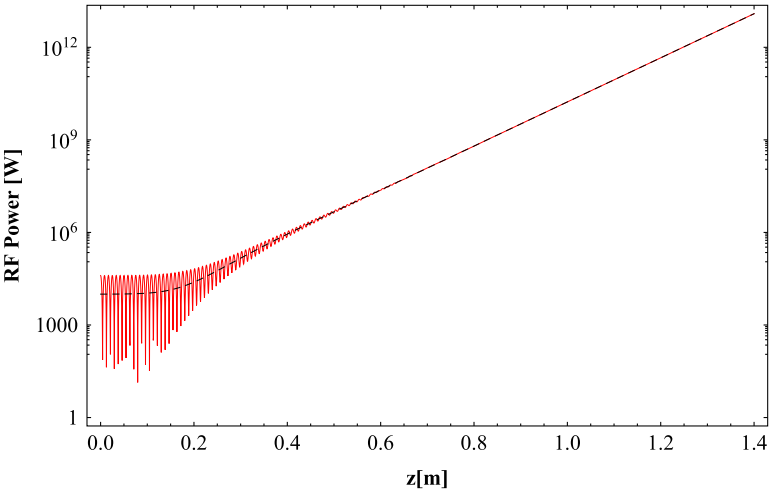

FIGURE 2. Small signal CARM growing intensity, with and without the imaginary contributions from (2.4).

$$A_2 := A_2(\bar{\nu}) = \frac{(2\nu + p + q)}{\nu + p + q}$$
$$= \frac{\left(\sqrt[3]{1 - 2\bar{\nu}^3 + \sqrt{1 - 4\bar{\nu}^3}} + \sqrt[3]{1 - 2\bar{\nu}^3 - \sqrt{1 - 4\bar{\nu}^3}} + 2\sqrt[3]{2}\bar{\nu}\right)}{\left(\sqrt[3]{1 - 2\bar{\nu}^3 + \sqrt{1 - 4\bar{\nu}^3}} + \sqrt[3]{1 - 2\bar{\nu}^3 - \sqrt{1 - 4\bar{\nu}^3}} + \sqrt[3]{2}\bar{\nu}\right)}, \tag{2.17b}$$

$$A_3^{(\pm)} := A_3^{(\pm)}(\bar{\nu}) = \frac{1}{\sqrt[3]{2}}\left(\sqrt[3]{1 - 2\bar{\nu}^3 + \sqrt{1 - 4\bar{\nu}^3}} \pm \sqrt[3]{1 - 2\bar{\nu}^3 - \sqrt{1 - 4\bar{\nu}^3}}\right), \tag{2.17c}$$

$$(p \pm q)\tau = \frac{\sqrt{3}}{\sqrt[3]{2}} 2\Gamma z \left(\sqrt[3]{1 - 2\bar{\nu}^3 + \sqrt{1 - 4\bar{\nu}^3}} \pm \sqrt[3]{1 - 2\bar{\nu}^3 - \sqrt{1 - 4\bar{\nu}^3}}\right)$$
$$= 2\sqrt{3}\Gamma z A_3^{(\pm)}. \tag{2.17d}$$

In figure 1 we have provided a comparison between the prediction of the CARM theory and of the U-FEL scaling equations, given in (2.11). The agreement is satisfactory and further comments will be given below.

We should put in evidence that the linear solution obtained solving the dispersion relation (2.2) has been regularized neglecting the oscillating root of the (2.4) as reported in figure 2 comparing the amplitude signal with and without the oscillating solution .

The following two remarks are in order to complete the previous discussion:

(i) The dispersion relations for CARM and U-FEL lead to a fourth and third degree algebraic equations respectively. This is a consequence of the fact that the CARM field equations have been derived without the assumption of paraxial approximation, while in the case of U-FEL the small signal problem is solved by the approximation of a slowly varying envelope (SVE). This assumption leads to a treatment involving algebraic equations of one degree lower. In adapting U-FEL to CARM theory, according to the prescription of this paper and of those

https://doi.org/10.1017/S0022377816001239 Published online by Cambridge University Press

reported in Ceccuzzi *et al.* (2015), we did not find particular differences, except for the initial part, where the SVE approximation smoothen the field oscillations. We must underline that the approximation of the dispersion equation with the elimination of the quasi resonant term is a further cause of the fluctuation at low intensities.

(ii) The equations (2.2)–(2.7) have been written without fixing the waveguide mode structure, we can however factorize the ε coupling parameter as the product of two terms, namely

$$\left.\begin{aligned} \varepsilon &= \Xi\, \mathrm{f}, \\ \mathrm{f} &= \frac{4\,\pi\,\beta_\perp^2}{\gamma\,\beta_z}\left(\frac{I_b}{I_A}\right), \end{aligned}\right\} \tag{2.18}$$

where $I_{b,A}$ denote the beam and Alfvén current, the parameter Ξ summarizes the details of the cavity mode and the effect due to the geometrical overlapping between electrons and waveguide modes.

This is not a secondary issue, in particular when the operation on higher-order transverse modes is foreseen. In this case the relevant spatial distribution is not provided by a Gaussian, covering smoothly the transverse surface, but by a kind of circular corona which demands an appropriate shaping of the transverse structure of the e-beam to optimize the coupling.

In figure 3 we have reported the gain length for different higher-order modes, along with the transverse mode distribution.

3. Numerical analysis, saturation and final comments

In the previous section we have developed quite a straightforward formalism to prove that most of the scaling formulae developed within the framework of FEL theory can be adapted to the study and design as well of CARM devices, at least for the case of the small signal regime.

In this section we include the nonlinear contributions and show that the logistic curve model (Artioli *et al.* 2012; Ceccuzzi *et al.* 2015) is an effective tool to study the evolution of the system up to the saturation.

We will provide a comparison of this analysis with the logistic growth model based on a family of S-shaped curves, the model has been shown to be very effective in reproducing the evolution of any system undergoing a dynamical behaviour ruled by an equation of the type

$$\frac{\mathrm{d}}{\mathrm{d}\,z}P = \frac{P}{l_g}\left[1 - \frac{P}{P_S}\right], \tag{3.1}$$

even though either CARM and U-FEL satisfy more complicated nonlinear equations for the growth of the power density. Equation (3.1) captures the essential physics of the problem, namely a linear growth followed by a quadratic nonlinearity when the power approaches P_S which denotes the saturated power. The solution of (3.1) can be written as

$$P\,(z) = P_0 \frac{\mathrm{e}^{z/l_g}}{1 + \dfrac{P_0}{P_S}\left[\mathrm{e}^{z/l_g} - 1\right]}, \tag{3.2}$$

where P_0 is the input radiation seed.

https://doi.org/10.1017/S0022377816001239 Published online by Cambridge University Press

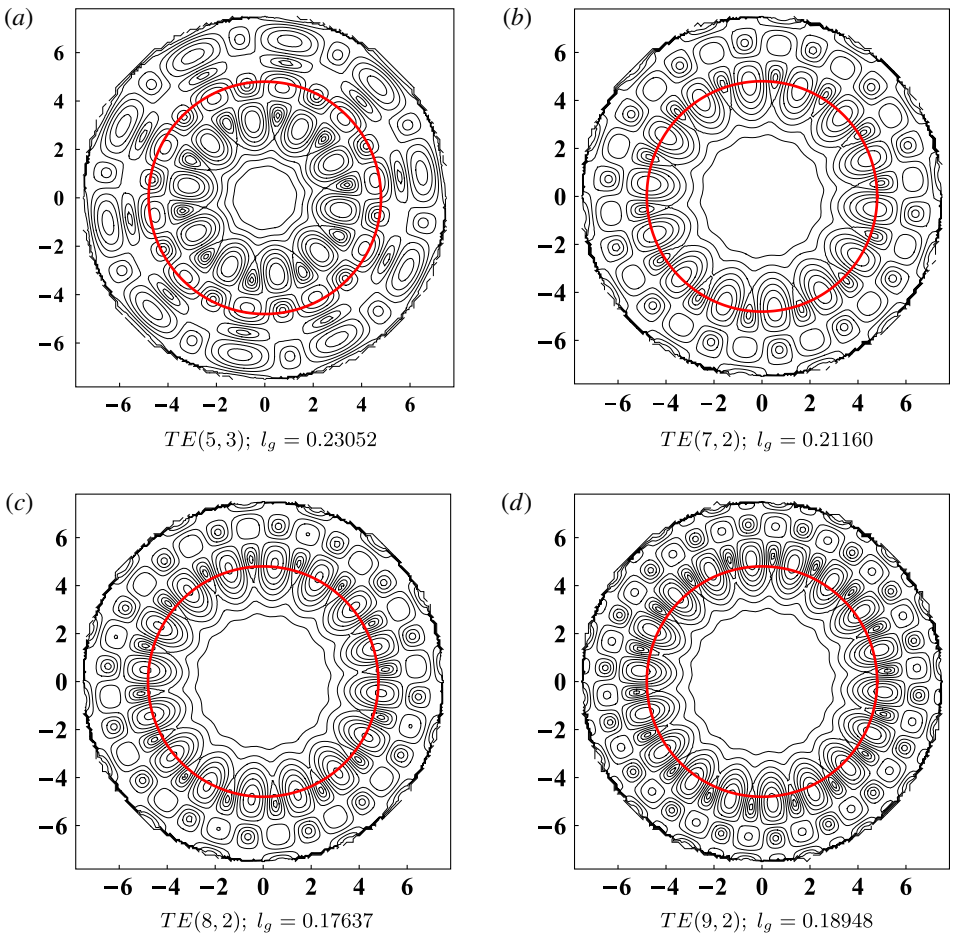

FIGURE 3. Transverse mode pattern and associated gain length. The circle in the middle represents the electron beam transverse distribution, which is assumed to stay well inside the mode itself thus maximizing the filling factor.

The definition of the CARM saturated power P_S is easily given by just following the prescriptions reported in Bratman *et al.* (1981), we set therefore

$$P_S \cong \eta\, P_E, \tag{3.3}$$

where P_E is the electron beam power and η the efficiency of the device in turn provided by

$$\eta = \eta_{sp}\eta_C, \tag{3.4}$$

where we have denoted by η_{sp} the single particle efficiency, (Bratman *et al.* 1981) which can be written using the analogy in terms of the Pierce parameter (Saldin *et al.* 2000; Dattoli *et al.* 2012) as

$$\eta_{sp} \cong \sqrt{2}\rho = \frac{\sqrt{2}\Lambda\,\Gamma}{4\,\pi\,\sqrt{3}}, \tag{3.5}$$

https://doi.org/10.1017/S0022377816001239 Published online by Cambridge University Press

while the collective efficiency η_C is specified by (Bratman *et al.* 1981)

$$\eta_C \cong \frac{1}{(1-\beta_p^{-2})\,(1-\gamma^{-1})}\frac{\beta_\perp^2}{b}, \quad \text{with } b = \frac{\beta_\perp^2}{2\,\beta_z\beta_p\left(1-\frac{\beta_z}{\beta_p}\right)}, \tag{3.6}$$

where, using the terminology of Bratman *et al.* (1981), b denotes the electron recoil parameter. It accounts for the auto resonance contribution, including the effect of axial momentum and velocity change with the electron energy loss (Bratman *et al.* 1981). Regarding the analogy with U-FEL it can be associated with the undulator tapering parameter (Kroll, Morton & Rosenbluth 1981; Dattoli *et al.* 2012).

According to the previous identity the saturated power can be cast in the form

$$P_S \cong \frac{\sqrt{2}}{4\pi\sqrt{3}}\frac{\Lambda\,\Gamma}{(1-\beta_p^{-2})\,(1-\gamma^{-1})}\frac{\beta_\perp^2}{b}P_E. \tag{3.7}$$

We have recovered all the crucial parameters (gain length and saturated power) to draw the CARM power growth curve using the logistic equation. However, equation (3.2) accounts only for the exponential growth prior to the saturation and does not contain any lethargic phase. To overcome this problem we replace the exponential term in (3.2) with the square modulus of the small signal amplitude derived in the previous section, thus writing

$$P(z) \cong P_0\frac{|\beta(z)|^2}{1+\frac{P_0}{P_S}\left(|\beta(z)|^2-1\right)} \quad \text{and} \quad \beta(\tau) = \frac{a(\tau(z))}{a_0}, \tag{3.8a,b}$$

with a_0 initial amplitude.

To check the validity of the previous formula we have developed an *ad hoc* numerical code to integrate the CARM equations (Gapanov *et al.* 1967; Bratman *et al.* 1979, 1981; Fliflet 1986; Chen & Wurtele 1991; Nusinovich *et al.* 1994).

The dynamical systems accounting for the evolution of CARM devices are described by a set of equations coupling electrons and field. From the mathematical point of view the problem is that of solving a system of nonlinear ordinary differential equation, consisting of four differential equations three of which account for the electron motion and the other for the complex field amplitude evolution inside the cavity, namely:

$$\frac{\mathrm{d}u}{\mathrm{d}\zeta} = \frac{[1-u]^{s/2}}{1-bu}Re(F_s\mathrm{e}^{-\mathrm{i}\theta}), \tag{3.9a}$$

$$\frac{\mathrm{d}\theta}{\mathrm{d}\zeta} = \frac{1}{1-bu}\left[\Delta-u-b\Upsilon(\zeta)+\frac{s}{2}[1-u]^{(s/2)-1}Re(\mathrm{i}F_s\mathrm{e}^{-\mathrm{i}\theta})\right], \tag{3.9b}$$

$$\frac{\mathrm{d}\Upsilon}{\mathrm{d}\zeta} = -\frac{[1-u]^{s/2}}{1-bu}Re\left(\mathrm{i}\frac{\mathrm{d}F_s}{\mathrm{d}\zeta}\mathrm{e}^{-\mathrm{i}\theta}\right), \tag{3.9c}$$

where the normalized u, θ, Υ variables are associated with the electron energy, the electron wavephase and the axial momentum correction respectively, s is the order of the harmonics, ζ is the normalized space variable and F_s accounts for the complex mode field amplitude, whose evolution is fixed by the equation

$$\frac{\mathrm{d}F_s}{\mathrm{d}\zeta} = I_g\left\langle\frac{[1-u]^{s/2}}{1-bu}\mathrm{e}^{\mathrm{i}\theta}\right\rangle, \tag{3.10}$$

https://doi.org/10.1017/S0022377816001239 Published online by Cambridge University Press

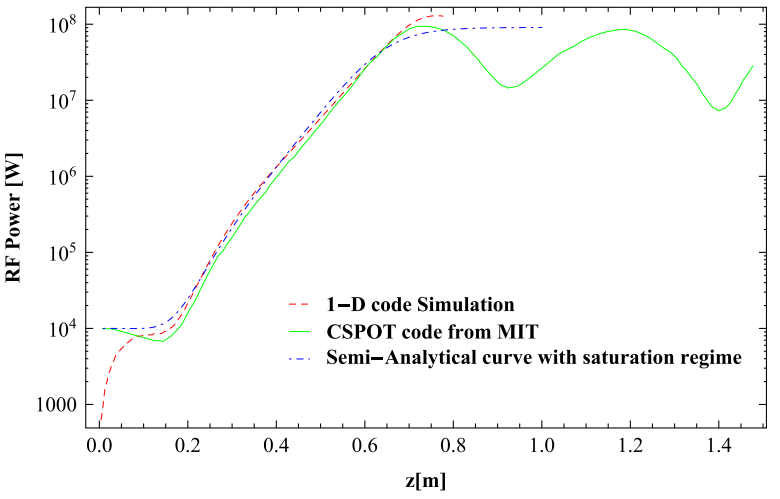

FIGURE 4. The revisited semi-analytical formula from FEL compared with numerical code.

with $\langle \cdots \rangle_{\theta_0}$ denoting the average taken on the initial phase distribution (Fliflet 1986; Dattoli *et al.* 1993; Nusinovich 2004; Ceccuzzi *et al.* 2015).

The pivotal parameters characterizing the previous equations system related to the CARM dynamics are summarized by three dimensionless quantities: b, accounting for the auto resonance, Δ, normalized detuning

$$\Delta = \frac{2\left(1-\frac{\beta_z}{\beta_p}\right)^2\left(1-\frac{\omega_R}{\omega}\right)}{\beta_\perp^2(1-\beta_p^{-2})}, \tag{3.11}$$

and I_g normalized beam current, proportional to the beam current I_b and expressible in terms of ρ parameter as

$$I_g = \left[\frac{4\sqrt[3]{2}\left(1-\frac{\beta_z}{\beta_p}\right)}{\beta_\perp^2\left(1-\beta_p^{-2}\right)}\rho\right]^3. \tag{3.12}$$

We will solve the previous set of equations valid, as already underscored, in the linear and nonlinear regimes and compare the result with the small signal analysis of the previous sections.

The adopted numerical procedure uses a Runge–Kutta scheme for the electron dynamics, with the field amplitude kept constant during one discretization step. Furthermore, a finite difference method has been applied to evaluate the differential equation concerning the amplitude wave evolution, in which the crucial step is the careful average of the electron phase distribution and the transverse velocity distribution in order to include correctly the effect of the beam qualities.

To study the effect of the particles velocity spread, starting form a fixed γ_0 beam energy and an α_0 pitch, a Gaussian distribution of the transverse velocity has been generated centred at the initial value of $\beta_{\perp 0}$.

https://doi.org/10.1017/S0022377816001239 Published online by Cambridge University Press

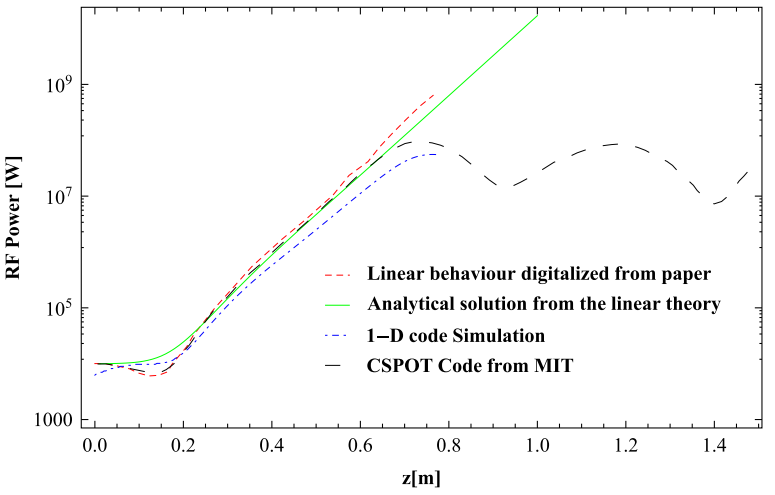

FIGURE 5. The analytical growth linear rate of the signal compared with the numerical simulation.

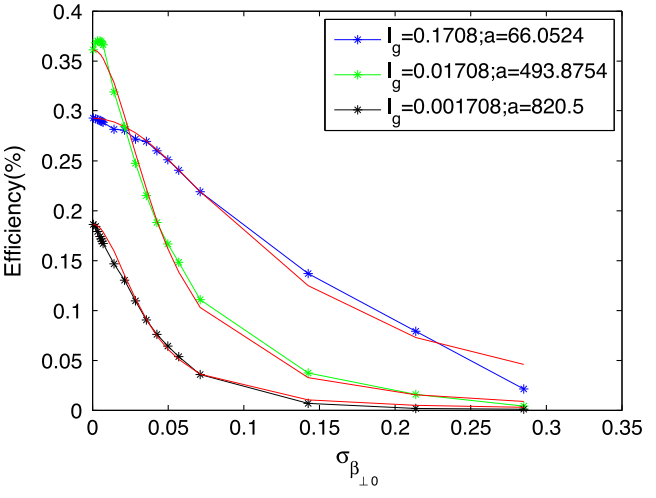

FIGURE 6. Efficiency behaviour (for optimal detuning Δ) versus transverse velocity spread for different values of I_g (dotted line numerical computation, red line Lorentzian fit).

For each particle we considered an ODE system characterized by a $b(\beta^i_{\perp 0})$ and $\Delta(\beta^i_{\perp 0})$ parameters and the integral average of the electron phase and velocity distribution have been evaluated by the use of a standard trapezoidal scheme.

Furthermore, the orbital efficiency has been obtained by averaging the electron motion on the electron phase and velocity distribution, allowing to evaluate the CARM power growth versus z as reported in figure 4.

The comparison between (3.8) and the power evolution obtained via the numerical implementation are shown in figures 4 and 5. The two curves compare fairly well; the use of these formulae for fixing the working points of a CARM device is therefore justified. The aim of the paper is to explore the analogy between CARM and U-FEL on the basis of a unifying common theoretical framework. This attempt is far from

https://doi.org/10.1017/S0022377816001239 Published online by Cambridge University Press

being exhaustive and the analogies should be exploited with care, for example we have not clarified whether the effects of beam quality on CARM performance can be accounted for by the 'universal' scaling formula as happens in the case of the U-FEL (Dattoli *et al.* 2007; Artioli *et al.* 2012).

The impact of the beam qualities on the CARM output power is shown in figure 6 where we have reported the power versus the root mean square of the transverse velocity ($\sigma_{\beta_\perp}$). The curves are nicely fitted by a Lorentzian ($\hat{\eta}_{sp} \propto (1/(1 + a\sigma^2_{\beta_\perp}))$, with $\hat{\eta}_{sp}$ the numerical single particle efficiency and a is a fit parameter), but a 'universal parameter' embedding inhomogeneous broadening effects and I_g (or ρ as well) has not been formulated yet. According to the suggestion put forward in Nusinovich *et al.* (1994) and later in Ceccuzzi *et al.* (2015) this seems to be possible, but further numerical analysis is needed to provide a more sound conclusion and is left for future investigations.

REFERENCES

Artioli, M., Dattoli, G., Ottaviani, P. L. & Pagnutti, S. Maggio-Giugno 2012 Virtual laboratory and computer aided design for free electron lasers outline and simulation. *Energia Ambiente e Innovazione* **3**, 128–132.

Bratman, V. L., Ginzburg, N. S. & Petelin, M. I. 1979 Common properties of free electron lasers. *Opt. Commun.* **30** (3), 409–412.

Bratman, V. L., Ginzburg, N. S., Nusinovich, G. S., Petelin, M. I. & Strklkov, P. S. 1981 Relativistic gyrotrons and cyclotron autoresonance maser. *Int. J. Electron.* **51** (4), 541–567.

Ceccuzzi, S., Dattoli, G., Di Palma, E., Doria, A., Sabia, E. & Spassovsky, I. 2015 The high gain integral equation for CARM-FEL devices. *IEEE J. Quantum Electron* **51** (7), 1–9.

Chen, C. & Wurtele, S. 1991 Linear and non linear theory of cyclotron autoresonance masers with multiple waveguide modes. *Phys. Fluids* **B 3**, 2133–2148.

Colson, W. B. 1990 Classical free electron laser theory. In *Free Electron Laser Handbook* (ed. W. B. Colson, C. Pellegrini & A. Renieri), pp. 115–194. North-Holland Physics, Elsevier.

Dattoli, G., Ottaviani, P. L. & Pagnutti, S. 2007 *Booklet for FEL Design: A Collection of Practical Formulae*. Edizioni Scientifiche Frascati.

Dattoli, G., Pagnutti, S., Ottaviani, P. L. & Asgekar, V. 2012 Free electron laser oscillators with tapered undulators: inclusion of harmonic generation and pulse propagation. *Phys. Rev. ST Accel. Beams* **15**, 030708.

Dattoli, G., Renieri, A. & Torre, A. 1993 *Lectures on the Free Electron Laser Theory and Related Topics*. World Scientific.

Fliflet, A. W. 1986 Linear and non-linear theory of the Doppler-shifted cyclotron resonance maser based on TE and TM waveguide modes. *Int. J. Electron.* **61** (6), 1049–1080.

Friedman, M., Hammer, D. A., Manheimer, W. M. & Sprangle, P. 1973 Enhanced microwave emission due to the transverse energy of a relativistic electron beam. *Phys. Rev. Lett.* **31** (12), 752–755.

Gapanov, A. V., Petelin, M. I. & Yulpatov, V. K. 1967 The induced radiation of excited classical oscillators and its use in high-frequency electronics. *Radiophys. Quantum Electron.* **10** (9), 794–813.

Kroll, N., Morton, P. & Rosenbluth, M. N. 1981 Free-electron lasers with variable parameter wigglers. *IEEE J. Quantum Electron.* **17**, 1436–1468.

Luchini, P. & Motz, H. 1990 *Undulators and Free-Electron Lasers*. Oxford University.

Marshall, T. 1985 *Free Electron Lasers*. Macmillan.

Nusinovich, G. 2004 *Introduction to The Physics of Gyrotrons*. The Johns Hopkins University Press.

Nusinovich, G. S., Latham, P. E. & Li, H. 1994 Efficiency of frequency up-shifted gyrodevices: cyclotron harmonics versus CARM's. *IEEE Trans. Plasma Sci.* **22** (5), 796–803.

Saldin, E., Schneidmiller, E. V. & Yurkov, M. V. 2000 *The Physics of Free Electron Lasers*. Springer.

https://doi.org/10.1017/S0022377816001239 Published online by Cambridge University Press